Materials Science & Engineering A 731 (2018) 119–123

Contents lists available at ScienceDirect

Materials Science & Engineering A

journal homepage: www.elsevier.com/locate/msea

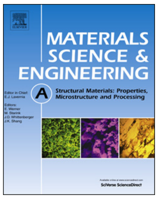

Exploring the correlation between the austenite yield strength and the bainite lath thickness

S.M.C. van Bohemen

Tata Steel Research Development and Technology, 1970 CA IJmuiden, The Netherlands

ARTICLE INFO

Keywords:
Austenite
Yield strength
Bainite
Lath thickness

ABSTRACT

The shape deformation associated with the formation of a bainite lath requires plastic accommodation in the neighboring austenite, and therefore it is assumed that the austenite yield strength will have a strong effect on the dimensions of the formed lath. Experimental data of the bainite lath thickness and the austenite yield strength have been examined to investigate this assumed dependency. First an equation is proposed to describe the austenite yield strength as a function of composition, grain size and temperature. This model has been validated with data of TWIP steels and medium carbon steels while also maintaining consistency with Irvine's original equation for austenitic stainless steels. Subsequently it is demonstrated that experimental data of the bainite lath thickness reported for various high-Si steels have an approximate inverse dependence with the austenite yield strength. On the basis of this correlation a concise model is proposed that can predict the bainite lath thickness as a function of composition, austenite grain size and temperature. Such a tool can be useful for alloy design in the development of new steels.

1. Introduction

The bainite lath thickness *t* has a major influence on the mechanical properties of bainitic steels [1,2], and therefore it is of key importance to understand the factors controlling the dimensions of a bainitic lath. The detailed information on the bainite lath thickness reported for various steels [1–10] stimulated the present study with the aim to describe the lath thickness as a function of both material and process parameters. Considering the fundamentals of the bainite transformation it is evident that the yield strength of austenite σ_y^γ plays an essential role because the shape deformation requires plastic accommodation of the bainite lath in the surrounding austenite [2,11]. Consistent with earlier studies [2,5] it is assumed in this investigation that σ_y^γ has a dominating effect on *t*.

For the data of fully austenitic substrates analysed in this study it is plausible to assume that precipitation and dislocation strengthening are insignificant, and therefore the austenite yield strength σ_y^γ can be written as [12]

$$\sigma_y^\gamma = \sigma_i + \sigma_s + \sigma_{gb} \quad (1)$$

in which σ_i represents the strengthening due to Peierls friction, σ_s describes solid solution strengthening effects of the alloying elements and σ_{gb} is given by the Hall-Petch relationship $\sigma_{gb} = K_{HP}\, d^{-1/2}$ and thereby accounts for the grain size effects.

In the first part of the paper Irvine's equation [12] describing the yield strength of austenitic stainless steels at room temperature will be assessed using TWIP steel data and accordingly the model will be modified to be applicable for a wider range of compositions. Furthermore, an equation will be proposed to calculated the temperature dependence of σ_y^γ which is based on the analysis of data of carbon steels for which σ_y^γ has been measured at elevated temperatures. In the second part of the paper it will be demonstrated that reported variations in *t* for various steels can be correlated to changes in σ_y^γ. Subsequently, a concise model will be derived to predict the bainite lath thickness as a function of composition, austenite grain size and temperature, which can be suitable in the design of new alloys.

2. Experimental data

2.1. The yield strength of TWIP steels

The derivation and validation of the proposed yield strength model is based on the data reported for TWIP steels in Refs [13,21]. The Appendix (Supplementary data) gives an overview of the compositions of all 34 TWIP steels from literature. The ranges of alloying, d^γ, and $\sigma_{y,25^\circ C}^\gamma$ are listed in Table 1.

2.2. Yield strength data of steels at elevated temperature

The yield strength data of various steels tested at elevated temperatures [22–25] were examined in order to determine an expression accounting for the reduction in σ_y^γ with increasing temperature. Table 2 shows the ranges of alloying, d^γ, T, and σ_y^γ. A full overview of the experimental data of these steels can be found in the Appendix (Supplementary data).

https://doi.org/10.1016/j.msea.2018.06.041
Received 18 April 2018; Received in revised form 22 May 2018; Accepted 11 June 2018

Table 1
Ranges of 34 data points from TWIP steels reported in literature [13–21].

	C wt%	Mn wt%	Al wt%	d^{γ} µm	exp. σ_y MPa
min.	0.02	12.0		3	155
max.	1.20	30.0	5.9	113	460

Table 2
Ranges of 16 data points from literature for tensile testing at elevated temperatures of various steels [22–25].

	C wt%	Mn wt%	Si wt%	Cr wt%	Mo wt%	Ni wt%	V wt%	d^{γ} µm	T °C	exp. σ_y MPa
min.	0.14		0.01					10	125	103
max.	0.96	2.69	2.08	16.30	1.48	24.90	0.93	100	700	324

2.3. *Bainite lath thickness data of various steels*

The bainite lath thickness data from Refs [6,10]. analysed in this study were all determined according to the same procedure. The mean linear L intercept was measured with the test line normal to the long edge of the plate, and subsequently the stereological correction $t = 2L/\pi$ was applied as described in Refs [7,26]. In Table 3 the experimental details of the steels from Refs [5,10]. are shown. The complete set of bainite lath thickness data can be found in the Appendix (Supplementary data).

3. Results and discussion

3.1. *Austenite yield strength*

The empirical relation describing the yield strength of stainless steels at room temperature, $\sigma^{\gamma}_{y,25^{\circ}C}$, proposed by Irvine et al. [12] was tested for various TWIP steels with carbon contents between 0.3 and 0.7 wt% [13–21]. The Irvine model has three strengthening contributions as described by Eq. (1). The assessment to the model led to predicted values of $\sigma^{\gamma}_{y,25^{\circ}C}$ being 10–25% higher than the experimental values, which means a discrepancy that is significantly higher than the typical experimental uncertainty in $\sigma^{\gamma}_{y,25^{\circ}C}$. The discrepancy can be explained by the fact that the parameters in Irvine's model [12] were optimized by fitting against experimental data of 88 different stainless

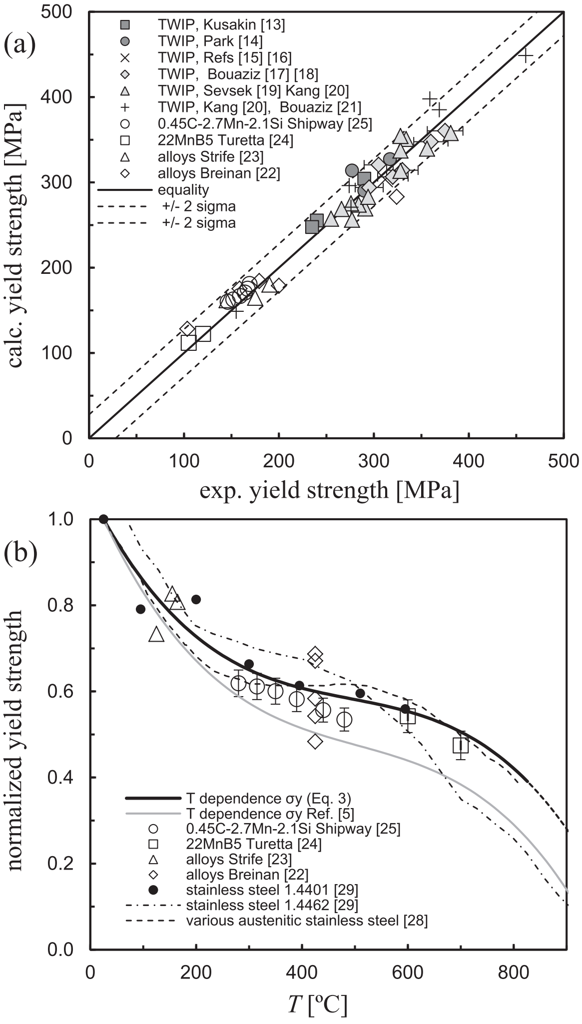

Fig. 1. (a) Correlation between the experimental austenite yield strength and values predicted with the proposed model (Eqs. (2) and (3)) and (b) the temperature dependence according to Eq. (3) compared to normalized yield strength data (symbols).

Table 3
Steels 1–11 used for model derivation, and steels 12–17 for verifying model predictions of the lath thickness.

No.	Ref.	Steel code (name in Reference)	C wt%	Mn wt%	Si wt%	Cr wt%	Mo wt%	Ni wt%	V wt%	Al wt%	Co wt%	d^{γ} µm	d^{γ} µm fit	$\sigma_{\lim}$ MPa fit	$\sigma_{\lim}$ MPa Eq. (5)
1	[6]	0.98C (1, 49 µm)	0.98	1.89	1.46	1.26	0.26		0.1			49		239	232
2	[6]	0.83C (2, 88 µm)	0.83	1.98	1.57	1.02	0.24				1.54	88		211	208
3	[6]	0.83C (2, 29 µm)	0.83	1.98	1.57	1.02	0.24				1.54	29		222	220
4	[6]	0.78C (3, 44 µm)	0.78	1.95	1.49	0.97	0.24			0.99	1.60	44		211	209
5	[6]	0.78C (3, 28 µm)	0.78	1.95	1.49	0.97	0.24			0.99		28		215	212
6	[5]	0.27C (alloy A)	0.27	2.18	1.98	1.90						24		141	142
7	[5]	0.46C (alloy C)	0.46	2.15	2.10							27		160	162
8	[5]	0.10C (alloy E)	0.10	2.12	1.77			2.0				65		100	102
9	[5]	0.26C (alloy F)	0.26	2.10	1.85							36		127	129
10	[5]	0.26C (alloy G)	0.26	2.04	1.93	1.02						18		144	135
11	[5]	0.10C (alloy H)	0.10	1.99	1.63	1.97						32		113	114
12	[7]	0.70C (Nano)	0.70	1.40	1.50	1.00	0.20	0.1					26		200
13	[7]	0.30C (Sub)	0.30	2.00	1.40	1.60	0.20	1.4		1.00	1.70		15		159
14	[8]	0.78C – 1.4Al	0.78	2.02	1.60	1.01	0.24			1.37	3.80		60		211
15	[9]	0.42C (A1, 920 °C)	0.42	2.37	1.50	1.41	0.25			0.82	1.40		95		151
16	[9]	0.42C (A1, 850 °C)	0.42	2.37	1.50	1.41	0.25			0.82	1.40		65		155
17	[9]	0.57C (A2, 920 °C)	0.57	2.02	1.52	1.21	0.24			0.65	1.60		75		174
18	[10]	1 C	1.02	0.75	1.49	0.44	0.02	0.1					55		233
19	[10]	1C-Co	0.99	0.76	1.58	0.46	0.02	0.1			2.50		55		235